Journal of Cellular and Molecular Medicine
A JOURNAL OF TRANSLATIONAL MEDICINE

J. Cell. Mol. Med. Vol 15, No 10, 2011 pp. 2245-2261

Infarcted myocardium-like stiffness contributes to endothelial progenitor lineage commitment of bone marrow mononuclear cells

Shuning Zhang [a, #], Aijun Sun [a, b, #], Hong Ma [a], Kang Yao [a], Ning Zhou [a], Li Shen [a], Chunyu Zhang [a], Yunzeng Zou [a, b] Junbo Ge [a, b, *]

[a] *Shanghai Institute of Cardiovascular Diseases, Zhongshan Hospital, Fudan University, Shanghai, China*
[b] *Institutes of Biomedical Sciences, Fudan University, Shanghai, China*

Received: June 17, 2010; Accepted: November 2, 2010

Abstract

Optimal timing of cell therapy for myocardial infarction (MI) appears during 5 to 14 days after the infarction. However, the potential mechanism requires further investigation. This work aimed to verify the hypothesis that myocardial stiffness within a propitious time frame might provide a most beneficial physical condition for cell lineage specification in favour of cardiac repair. Serum vascular endothelial growth factor (VEGF) levels and myocardial stiffness of MI mice were consecutively detected. Isolated bone marrow mononuclear cells (BMMNCs) were injected into infarction zone at distinct time-points and cardiac function were measured 2 months after infarction. Polyacrylamide gel substrates with varied stiffness were used to mechanically mimic the infarcted myocardium. BMMNCs were plated on the flexible culture substrates under different concentrations of VEGF. Endothelial progenitor lineage commitment of BMMNCs was verified by immunofluorescent technique and flow cytometry. Our results demonstrated that the optimal timing in terms of improvement of cardiac function occurred during 7 to 14 days after MI, which was consistent with maximized capillary density at this time domains, but not with peak VEGF concentration. Percentage of double-positive cells for DiI-labelled acetylated low-density lipoprotein uptake and fluorescein isothiocyanate (FITC)-UEA-1 (ulex europaeus agglutinin I lectin) binding had no significant differences among the tissue-like stiffness in high concentration VEGF. With the decrease of VEGF concentration, the benefit of 42 kPa stiffness, corresponding to infarcted myocardium at days 7 to 14, gradually occurred and peaked when it was removed from culture medium. Likewise, combined expressions of $VEGFR2^{+}$, $CD133^{+}$ and $CD45^{-}$ remained the highest level on 42 kPa substrate in conditions of lower concentration VEGF. In conclusion, the optimal efficacy of BMMNCs therapy at 7 to 14 days after MI might result from non-VEGF dependent angiogenesis, and myocardial stiffness at this time domains was more suitable for endothelial progenitor lineage specification of BMMNCs. The results here highlight the need for greater attention to mechanical microenvironments in cell culture and cell therapy.

Keywords: bone marrow-derived mononuclear cells • differentiation • elastic modulus • endothelial progenitor cells • myocardial infarction

Introduction

Time-dependent therapeutic response exists in cell-based cardiac repair after myocardial infarction (MI) [1]. Results from clinical or experimental research have shown that the optimal time frame for bone marrow-derived cell therapy for MI might be day 5 to week 2 after the infarction [2–4]. However, the potential mechanism has remained largely unexplored. Early transplanted cells do not survive in this milieu, most likely in view of the hostile environment in the first days after MI. Thus, suitable microenvironment around transplanted cells within infarcted myocardium, might play an essential role in deciding the optimal timing of cell therapy.

There is accumulating evidence to demonstrate that stem cells are able to feel and respond to the physical factor (usually called 'stiffness' or 'elasticity') of their microenvironment to commit to a relevant lineage. Soft matrices (elastic modulus, *E*, a material property that describes its stiffness or elasticity, 0.1~1.0 kPa) that mimic brain are neurogenic, stiffer matrices (*E* ~11 kPa) that

[#]These authors contributed equally to this work.
*Correspondence to: Junbo GE, M.D., F.A.C.C., F.E.S.C., F.S.C.A.I., Shanghai Institute of Cardiovascular Diseases, Zhongshan Hospital, Fudan University, 180 Fenglin Road, Shanghai 200032, China.
Tel.: +86–21-64041990
Fax: +86–21-64223006
E-mail: jbge@zs-hospital.sh.cn

doi: 10.1111/j.1582-4934.2010.01217.x

mimic muscle are myogenic, and comparatively rigid matrices (E ~34 kPa) that mimic collagenous bone prove osteogenic [5]. That is to say, stem cell differentiation is highly sensitive to tissue-like stiffness, as well as the cellular phenotype and biological behaviour after differentiation may more closely mimic that of the cells in their normal host tissue.

Associating these findings with the fact that the infarcted myocardium experiences time-dependent stiffness changes from flexible to rigid due to myocardial remodelling following the tissue necrosis and massive extracellular matrix deposition [6–7], we have suggested previously that myocardial stiffness within the optimal treatment time domains might offer the most beneficial physical microenvironment in promoting phenotypic plasticity and functional specification of engrafted cells along endothelial lineages, especially endothelial progenitor cells (EPCs), which facilitated angiogenesis and, therefore, resulted in cardiac repair and amelioration of cardiac functions [8]. The work here attempts to verify the hypothesis and *in vitro* accesses the effects of the stiffness of infarcted myocardium on the specification of bone marrow-derived cells along endothelial progenitor lineage.

Materials and methods

Animal models

Male Balb/c mice were 6 weeks of age at the start of the experimental protocol. Mouse models of MI were prepared by the ligation of the left anterior descending artery as described previously [9]. Briefly, a thoracotomy was performed through the fourth left intercostal space, and the proximal left anterior descending artery was permanently ligated by a 8.0 silk suture. Control animals only underwent thoracotomy. All animal experiments were performed in accordance with the National Institutes of Health Guide for the Care and Use of Laboratory Animals (NIH Pub. No. 86–23, revised 1996) and with the approval of the Animal Care Committee of Zhongshan Hospital, Fudan University, China.

Measurement of serum vascular endothelial growth factor (VEGF) levels and histological staining

Twenty experimental mice were killed consecutively at 1 hr, 24 hrs, 7 days, 14 days and 28 days after the procedure by exsanguinations under ketamine anaesthesia. The blood serum was collected and kept frozen at –20°C until evaluation ($n = 4$ per time-point). Serum concentrations of VEGF were detected by ELISA technique, as manufacturer's protocol (RapidBio, Inc., Calabasas, CA, USA). Thereafter the hearts were dissected carefully and fixed in freshly prepared 4% paraformaldehyde for histological staining. The left ventricle was cut in two halves through the centre of the infarct vertical to the longitudinal axis. Paraffin sections from the infarct centre were stained with haematoxylin and eosin and Mallory's trichrome. The percentage of blue staining indicated the extent of fibrosis. All images were obtained at 400× using inverted optical microscope (TS100; Nikon, Corp., Tokyo, Japan).

Isolation of mouse bone marrow mononuclear cells (BMMNCs)

Femurs from male Balb/c mice of 6 weeks of age were flushed three times in phosphate-buffered solution (PBS) with 26G needle to collect bone marrow cells. BMMNCs were isolated by density gradient centrifugation using Ficoll (Sigma-Aldrich, St. Louis, MO, USA) as an established protocol [10]. Briefly, three microlitres of cell suspension was carefully lay over 3 ml of Ficoll-Paque in a 15 ml conical tube. Thereafter it was centrifuged at 2000 rounds per minute for 30 min. at 4°C. The mononuclear cell layer at the interphase was aspirated undisturbed and transferred to a new 15 ml conical tube. Isolated cells were washed twice and resuspended in complete M199 culture medium (Gibco BRL., Rockville, MD, USA).

Intramyocardial cell injection

At 1 hr after MI, experimental mice were re-anaesthetized and echocardiography performed. Forty animals with comparable body weight and reduced ejection fraction (<65%) were then randomly divided into four groups (1 hr, 24 hrs, 7 days and 14 days group; 28 day group was deleted from the work because infarction zone was too thin to perform cell transplantation). In each group, 10 of the animals were randomly designed to receive DiI-labelled BMMNCs injection or M199 medium injection in infarcted area (3 sites) with a total volume of 2 μl containing 4×10^4 cells or M199 medium (isolation of BMMNCs). Two months after the infarction, five animals in each subgroup (cell treatment subgroups and M199 injection subgroups) were further studied to blindly assess left ventricular function and pressure, as well as were then killed for detecting capillary density in the injected areas.

Detection of cardiac function and left ventricular pressure

Echocardiography was conducted using VisualSonic high-resolution micro-imaging system (Vevo770; VisualSonic, Inc., Toronto, Canada) equipped with a linear 30 MHz probe (RMV 707B) at 2 months after MI in each group. Animals were induced with isoflurane, received continuous inhaled anaesthetic (1%) for the duration of the imaging session, and were imaged in the supine position. M-mode long-axis views of the left ventricle were obtained and archived. Ejection fraction, fractional shortening (FS), left ventricular end-diastolic diameters (LVEDd), and left ventricular end-systolic diameters (LVEDs) were measured. During data collection, heart rates remained at 400 to 500 beats per minute. Analysis of images was performed with Vevo770 version 3.0.0 analysis software (VisualSonic, Inc.). All measurements were averaged for three consecutive cardiac cycles.

Left ventricular pressure was evaluated by pressure–volume conductance catheter technique (Millar, Inc., Houston, TX, USA), as described previously [11]. Briefly, mice were anaesthetized with ketamine, 100 mg/kg, intraperitoneally. A vertical midline cervical incision was made to expose the trachea. The right carotid artery and external jugular vein were exposed *via* the same midline incision. A 1.4 F Millar catheter was advanced *via* the right carotid artery into the ascending aorta and then inserted into left ventricle for measurements of left ventricle pressure. The data were recorded as left ventricular end-diastolic/systolic pressure and slope of derivative of change in systolic/diastolic pressure over time (±dP/dt) curves for 5 min.

During data collection, heat rates remained at 400 to 500 beats per minute. Analysis of images was performed with Chart 5 software (ADInstruments, Inc., Sydney, Australia). All measurements were averaged for 10 stable consecutive cardiac cycles.

Capillary density in the injection area

The engrafted cells were identified by the presence of DiI^+ cells in frozen sections made from hearts with MI. Unfortunately, DiI^+ cells were not found in cell injection zone probably due to fluorescent quenching as a result of long period from cell injection to cell identification. Capillary density in the transplanted area was detected by observing the expression of vWF (anti-human antibody; Dako, Copenhagen, Denmark) using immunohistochemical method. The number of vessel was evaluated by counting five randomly chosen high-power fields (HPF, 400×) from each of five sections taken from each animal. The number of capillary in each was averaged and expressed as the number of capillary per HPF.

Stiffness probing for infarcted myocardium

The fresh hearts after MI were dissected and stored in 0.9% sodium chloride solution ($n = 4$ per time-point) for stiffness probing. Heart sections were prepared and the elastic moduli were measured essentially as described by Berry et al. previously [7]. Briefly, infarcted and control tissue from experimental animals was sectioned parallel to the longitudinal axis of the left ventricle from the vascular ligation point to cardiac apex to yield tissue samples ~0.5 mm thick. Thereafter the septal surface was mounted and immobilized on coverglass with adhesive tape, exposing the lateral surface for probing. Tissue samples were placed on an atomic force microscope (Nanoscope IIIa; Digital Instruments, Inc., USA), and indented by a pyramid-tipped cantilever with spring constant of 60 pN/nm (Nanoprobes, Inc., Yaphank, NY, USA) using a contact mode in fluid. Mechanical information at 10 positions per sample was obtained and at each position five force–indentation plots were recorded. NanoScope software 5.30 (Veeco Instruments, Inc., Plainview, NY, USA) was used to acquire images. Elastic modulus was calculated based on the formula previously described by Domke [12].

In vitro mimicry of myocardial stiffness and preparation of cell culture dishes

The variably compliant polyacrylamide gels were prepared according to a previously established protocol by Pelham and Wang [13]. Polyacrylamide gel substrates were polymerized as thin films on a ~20 mm round glass bottom, a part of ~35 mm cell culture dish (Shengyou, Inc., Hangzhou China). To induce bisacrylamide crosslinking, 10% ammonium persulphate and N,N,N′,N′-tetramethylethylenediamine were added to polyacrylamide gel solutions, composed of 5–8% acrylamide monomer and 0.02–0.12% bisacrylamide crosslinker. Drops of polymerizing gel solution were added on the glutaraldehyde-treated aminosilanized round glass bottom with three 1 × 1 mm rectangular glass slips around it. Chlorosilanized round cover-slips (~18 mm) were placed on top of the polyacrylamide, and weights were added to ensure that the gel thickness was defined by that of the rectangular glass slips. Thereafter elastic modulus of the prepared gels was detected using atomic force microscopy in liquid conditions of 0.9% sodium chloride solution. Among the force measurements, we sieved those which matched with mechanical characteristics of infarcted myocardium at the above designated time-points. Human fibronectin (Biosource, Camarillo, CA, USA) was chemically crosslinked to polyacrylamide gel using a heterobifunctional photoactivating crosslinker, sulfo-SANPAH (Thermo Fisher Scientific, Inc., Rockford, IL, USA) [14]. Before being used for cell culture, the gels covered with PBS were exposed to ultraviolet ray with wavelength of 275 nm for 15 min. Thereafter PBS was replaced with complete M199 culture medium (with 10% foetal bovine serum) and cell culture dishes were placed in incubator for 2 hrs to allow equilibrium.

Culture of mouse BMMNCs

Isolated cells were resuspended in complete M199 culture medium (Gibco) with different concentrations of VEGF (0 ng/ml, 2.5 ng/ml, 10 ng/ml, 20 ng/ml) (VEGF; Peprotech, Inc., Rocky Hill, NJ, USA). Then BMMNCs were seeded at a density of 1×10^6 cells/dish in a ~20 mm culture dish with the flexible substrate, and were maintained in humidified air with 5% CO_2 at 37°C. After 48 hrs in culture, non-adherent cells were removed and adherent cells were cultured continuously. Culture medium was changed every 48 hrs.

Acetylated low-density lipoprotein uptake and ulex europaeus lectin binding

EPCs were characterized as adherent cells double positive for DiI-labelled acetylated low-density lipoprotein (DiI-acLDL) uptake and FITC-labelled ulex europaeus agglutinin I lectin (FITC-UEA-1) binding. After 7 days in culture, adherent cells were incubated with 10 μg/ml DiI-acLDL (Biomedical Technologies, Inc., Stoughton, MA, USA) in serum-free M199 culture medium at 37°C for 3 hrs. Cells were fixed with 4% formaldehyde for 15 min. and subsequently stained with FITC-UEA-1 (Sigma) for 2 hrs at room temperature. Nuclei were counterstained with 1 μg/ml 4,6-Diamidino-2-phenylindole (Roche, USA) for 10 min. at room temperature. Samples were viewed with a laser scanning confocal microscope (LSM510; Carl Zeiss, Jena, Germany). Five images per cultured cell sample were collected at 200× magnification and the percentages of FITC-UEA-1/ DiI-acLDL double-positive cells were calculated based on the images, as well as the positive cell number per HPF (400× magnification) based on the double-positive ratio. To assess reproducibility of the measurements, three separate tests were conducted.

EPCs-specific surface antigens expression

Adherent cells were trypsinized and EPCs-specific surface antigens were identified and quantified using fluorescence-activated cell sorter analysis (Epics Altra; Beckman Coulter, Inc., Brea, CA, USA), as described previously [15]. The cells were immunostained with phycoerythrin (PE)-labelled anti-mouse CD133 antibody, APC-labelled anti-mouse VEGFR2 antibody, and FITC-labelled anti-mouse CD45 antibody (eBioscience, San Diego, CA, USA) per manufacturer's protocol. Furthermore, cells were labelled with the following fluorescent antibodies: PE-labelled IgG 2a, APC-labelled IgG 2a and FITC-labelled IgG 2a (eBioscience) as isotype controls. Data were analysed using the EXPO32 V1.2 Analysis software (Beckman Coulter, Inc.).

Statistical analysis

Continuous variables were presented as mean and standard error values. Statistical comparisons between cell treatment groups and M199 injection

groups were made by analysis of variance with Student's t-test. Comparisons of left ventricular parameters among cell treatment groups were based on the absolute change from the respective control (M199 injection group) (presented as δ values). Intergroup analyses were conducted using ANOVA. Two-way ANOVA was used to detect the co-effects of matrix stiffness and VEGF on endothelial progenitor lineage specification of BMMNCs. *P*-values <0.05 were considered significant. Data analyses were performed by SPSS 11.5 software (SPSS, Inc., Chicago, IL, USA).

Results

Time-related changes in stiffness and tissue pathology of infarcted myocardium as well as serum VEGF level

There was no significant change in the stiffness of myocardium at 1 hr after MI compared to that of normal myocardium ($E = 16.60 \pm 0.40$ kPa *versus* 17.94 ± 0.39 kPa, $P > 0.05$; Fig. 1A, B, G). After 24 hrs, the elastic modulus of infarcted myocardium decreased to the lowest level ($E = 4.21 \pm 0.16$ kPa, *versus* that of normal myocardium, $P < 0.001$; Fig. 1A, C, G). Thereafter the stiffness of infarcted myocardium gradually increased and there were statistically significant differences in comparison with normal myocardium (day 7 after MI: $E = 31.38 \pm 0.75$ kPa; day 14: $E = 53.23 \pm 0.75$ kPa; day 28: $E = 90.22 \pm 2.97$ kPa; all $P < 0.001$; Fig. 1A, D–G).

The time-related changes in stiffness of infarcted myocardium might be closely associated with the pathological changes following MI. Hearts at hour 24 after MI had more significant inflammatory cells infiltration following massive myonecrosis, which could account for the phenomenon of myocardial stiffness decreasing to the lowest level at this time (Fig. 1C). By day 7, the removal of the necrotic myocytes was paralleled by a reduction of inflammatory cells with the start of immature fibrosis scar formation. And the process completed by 28 days after MI. The fibrotic process might greatly contribute to the time-related increase in the stiffness of infarcted myocardium (Fig. 1D–F).

Serum VEGF significantly increased at 1 hr after MI compared with sham group (49.44 ± 2.20 pg/ml *versus* 38.58 ± 1.32 pg/ml, $P = 0.02$) and reached peak concentration by hour 24, with statistically significant differences (96.30 ± 8.87 pg/ml, $P < 0.01$). Thereafter serum VEGF concentration gradually decreased and reached the sham group level by day 14 after MI (43.89 ± 4.66 pg/ml, $P > 0.10$, Fig. 2).

Cardiac function recovery after cell treatment

Compared with the M199 injection at respective time-points, cell treatment at hour 24, day 7 and day 14 after MI significantly improved LVEF, FS, left ventricular end-diastolic pressure (LVEDP) and $\pm$dp/dt after the infarction (Fig. 3A1, B1; Fig. 4A1, C1, D1). Comparisons of absolute changes from respective control data among all cell-treat groups demonstrated the more benefits in terms of LVEF, FS, LVEDP and $+$dp/dt in 7 day group and 14 day group than other groups (Fig. 3A2, B2; Fig. 4A2, D2). The effects of cell transplantation on the above parameters were more favourable in 7 day group than 24 hr group (all $P < 0.05$), whereas there were no significant differences between day 7 injection group and day 14 injection group (all $P > 0.05$). However, except for 7 day group in which there existed significant decreases in LVEDd/s compared with the control, the benefits associated with cell treatment were not presented in LVEDd/s and LVESP regardless of intra- or inter-group comparisons. Nevertheless, cell treatment at 7 days and 14 days after the infarction still showed favourable tendencies to improve these anatomic parameters compared with those at other time-points, although no significant differences (Fig. 3C2 and D2).

Density of vessels in cell injected zone

Capillary density within cell transplantation area in 24 hr, 7 day and 14 day group was more than that in M199 injection group (M199 group: 1.32/HPF; 24 hr, 7 day, 14 day group: 2.60 /HPF, 4.60/HPF, 3.80/HPF, respectively; all *P*-value <0.01). There was no significant difference between 1 hr treatment group and M199 group ($P > 0.05$, Fig. 5). Among all the injection groups, 7 day and 14 day groups had the highest capillary density. However, no difference was demonstrated between the two groups.

In vitro mimicry of the stiffness of infarcted myocardium

We precisely measured the elastic modulus of eight thin gel films by atomic force microscope, and from which four matrix gels with infarcted myocardium-like stiffness were selected as the substrates for cell culture. Elastic modulus of the bolted gels were 3.83 ± 0.49 kPa (regarded as ~4 kPa), 15.47 ± 0.78 kPa (~15 kPa), 42.62 ± 0.66 kPa (~42 kPa) and 72.15 ± 1.28 kPa (~72 kPa) (Fig. 6), which could *in vitro* mimic that of myocardium at hour 24, hour 1, days 7 to 14 and days 14 to 28 after the infarction (Fig. 1G), respectively.

Identification of endothelial progenitor characteristics of BMMNCs under culture conditions of infarcted myocardium-like stiffness

On day 7 after culture, the percentage and number of double-positive cells for FITC-UEA-1 binding and DiI-acLDL uptake had no significant differences among the infarcted myocardium-like stiffness under condition of 20 ng/ml VEGF ($P > 0.05$) (Fig. 7). When the culture condition was changed to 10 ng/ml VEGF, the stiffness of 42 and 15 kPa, corresponding to myocardium at

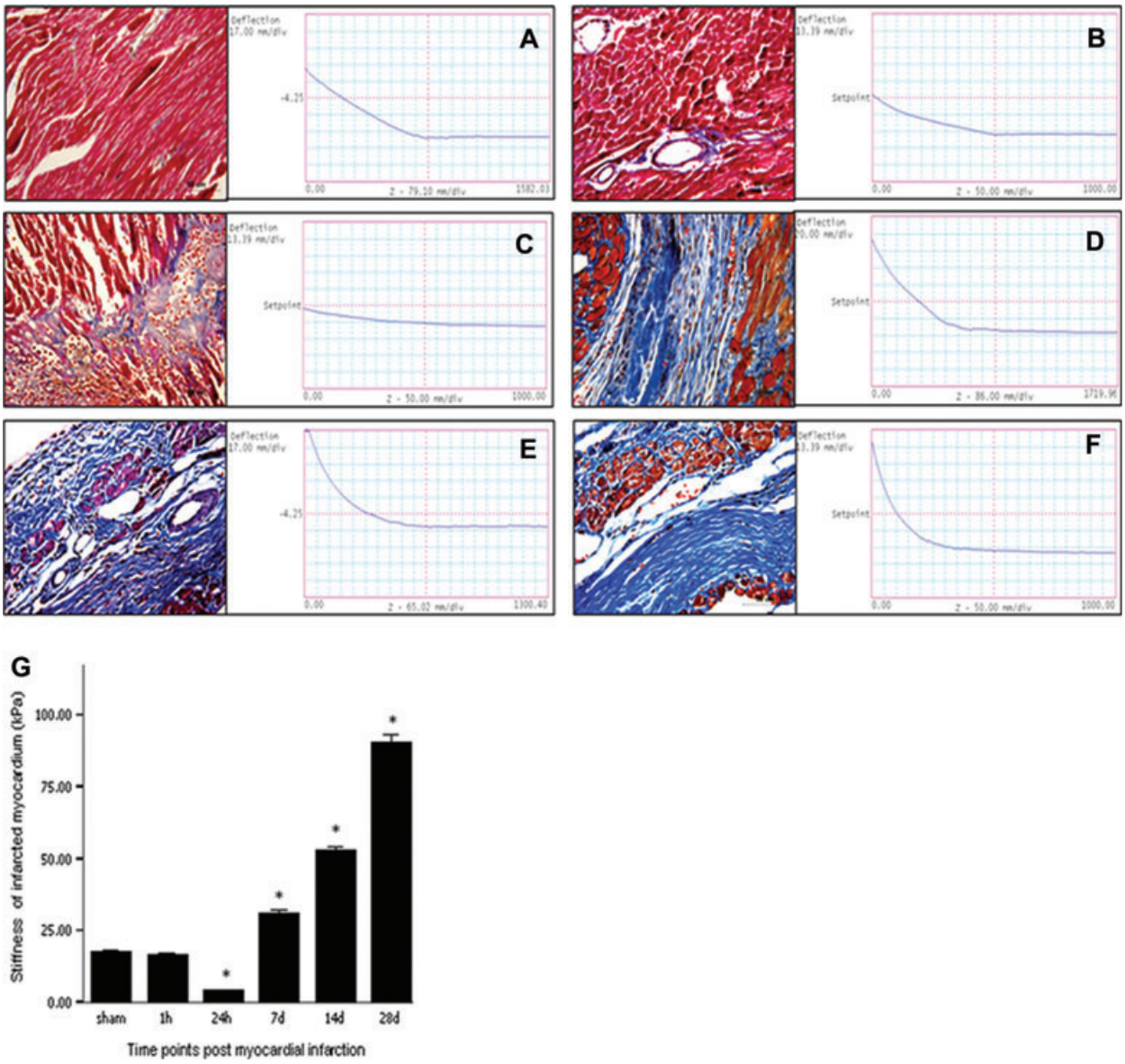

Fig. 1 Time-related changes in myocardial stiffness (**A**–**F**, right; **G**) and pathological staining (**A**–**F**, left) of the infarcted myocardium. (**A**) normal myocardium; (**B**) infarcted myocardum at hour 1; (**C**) infarcted myocardum at hour 24; (**D**) infarcted myocardum at day 7; (**E**) infarcted myocardum at day 14; (**F**) infarcted myocardum at day 28. Bars mean S.D. $*P < 0.05$ *versus* group A.

days 7 to 14 and hour 1 after MI, respectively, showed significant benefits only in the number of double-positive cells per HPF (Fig. 8). With the further decrease of VEGF concentrations to 2.5 ng/ml, the difference in the percentage of double-positive cells started to be statistically significant between 42 and 15 kPa (72.44% *versus* 52.44%, $P = 0.04$). Meanwhile, a more double-positive cell number was shown in the stiffness of 42 kPa compared with other flexibility (Fig. 9). Interestingly, when VEGF was removed from the culture medium, the beneficial differences in the percentage and number of FITC-UEA-1/DiI-acLDL double-positive cells between the stiffness of 42 kPa and other elasticity became maximized, with statistical signification or quasi-signification (cell percentage: 70.50% *versus* 4 kPa: 45.00%, $P = 0.01$; *versus* 15 kPa: 38.00%, $P = 0.005$; *versus* 72 kPa: 54.50%, $P = 0.06$; cell number: 167/HPF *versus* 4 kPa: 67/HPF, $P = 0.002$; *versus* 15 kPa: 73/HPF, $P = 0.008$; *versus* 72 kPa: 64/HPF, $P = 0.003$) (Fig. 10). In addition, the co-effects of infarcted myocardium-like stiffness and VEGF concentrations on inducing endothelial progenitor lineage specification of BMMNCs were demonstrated in the present research ($P < 0.01$). In two-way ANOVA, the stiffness of 42 kPa still

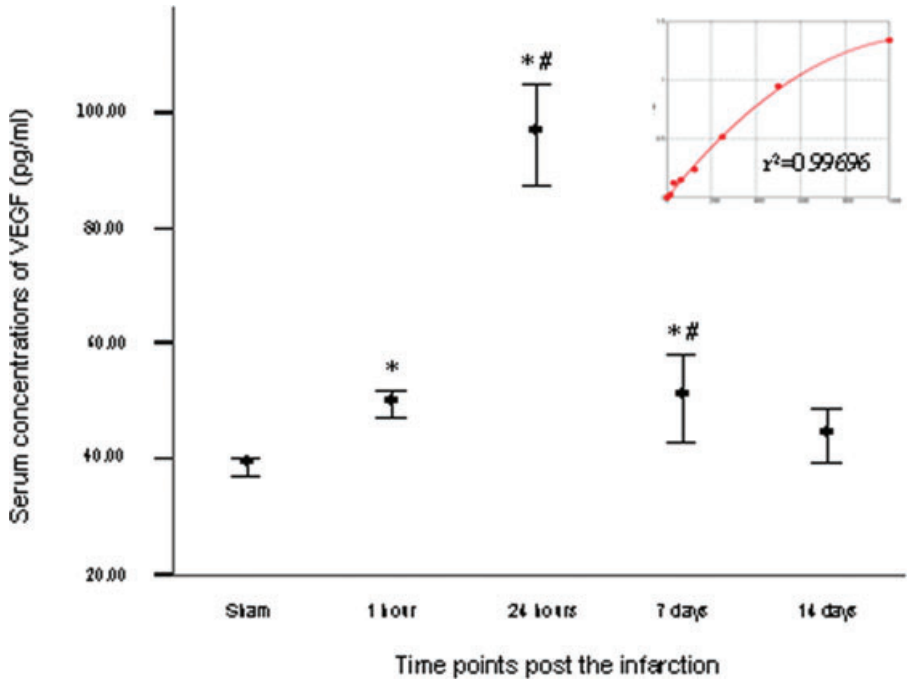

Fig. 2 Serial changes in serum concentration of VEGF after MI. Bars mean standard errors. $*P < 0.05$ *versus* sham group; $\#P < 0.05$ *versus* left neighbour.

showed the more benefits in terms of the percentage and number of FITC-UEA-1/DiI-AcLDL double-positive cells after controlling the impacts of VEGF concentrations (Fig. 11A). Unexpectedly, lower VEGF concentration (2.5 ng/ml) seemed likely to contribute to the higher percentage and more number of double-positive cells irrespective of the tissue-like stiffness (Fig. 11B).

Based on the benefits of lower concentration of VEGF, we next tested whether the stiffness of culture substrates also guided the single and combined expressions of EPCs-specific surface antigens, $VEGFR2^+$, $CD133^+$ and $CD45^-$, in the medium with 2.5 ng/ml VEGF. Indeed, flow cytometry similarly revealed that the stiffness of 42 kPa gave rise to a higher expression of VEGFR2 in BMMNCs (11.5% *versus* 4 kPa : 8.8%, 15 kPa: 6.6%, 72 kPa: 5.6%) (Fig. 12A). Combined expressions of $VEGFR2^+$, $CD133^+$ and $CD45^-$ also remained the highest level in 42 kPa substrate (1.94% *versus* 4 kPa: 0.68%, 15 kPa: 0.48%, 72 kPa: 0.79%) (Fig. 12B).

Discussion

In an attempt to verify the hypothesis that time-related stiffness of myocardium after the infarction might play an important role in guiding commitments of engrafted cells to some cell lineages in favour of cardiac repair [8], results here demonstrated that infarcted myocardium-like rigidity is sufficient to induce endothelial progenitor lineage specification of BMMNCs. Concretely, the recovery of cardiac function was significantly more when cell injection was performed at 7 to 14 days *versus* 1 to 24 hrs after MI, which was consistent with the observation of capillary density in the injection zone. And the stiffness of 42 kPa, corresponding to infarcted myocardium at days 7 to 14, was more suitable for BMMNCs' double fluorescent staining with FITC-UEA-1 and DiI-acLDL, as well as combined expressions of $VEGFR2^+$, $CD133^+$ and $CD45^-$, which were the unique characteristics of EPCs. The observations indicated that the myocardium at weeks 1 to 2 after MI might offer the optimal physical microenvironment for commitments of engrafted pluripotent cells to EPCs. The stiffness-dependent effects appeared to be strongly impacted by VEGF concentrations. The differences among the flexibility vanished under conditions of high concentration of VEGF (20 ng/ml). Conversely, the benefits of 42 kPa stiffness became maximized when VEGF was removed from the culture medium.

BMMNCs contain pluripotent stem cells and progenitor cells, which have the potential to multiply and differentiate in both contractile and blood-vessel cells [16–17]. These beneficial effects are in favour of broken heart repair and functional recovery [16]. In an animal experiment BMMNCs exhibit a more favourable survival pattern which translates into a more robust preservation of cardiac function compared to mesenchymal stem cells, skeletal myoblasts and fibroblasts [17]. Currently BMMNCs have become the most widely used cell populations in clinical practices [3, 18]. BMMNCs fate after transplantation contributed largely to cell efficacy. Neovascularization of ischemic cardiac may be sufficient to preserve tissue integrity or function and may thus be considered as a therapeutic goal [19]. Recently, Yoon *et al.* [20] demonstrated

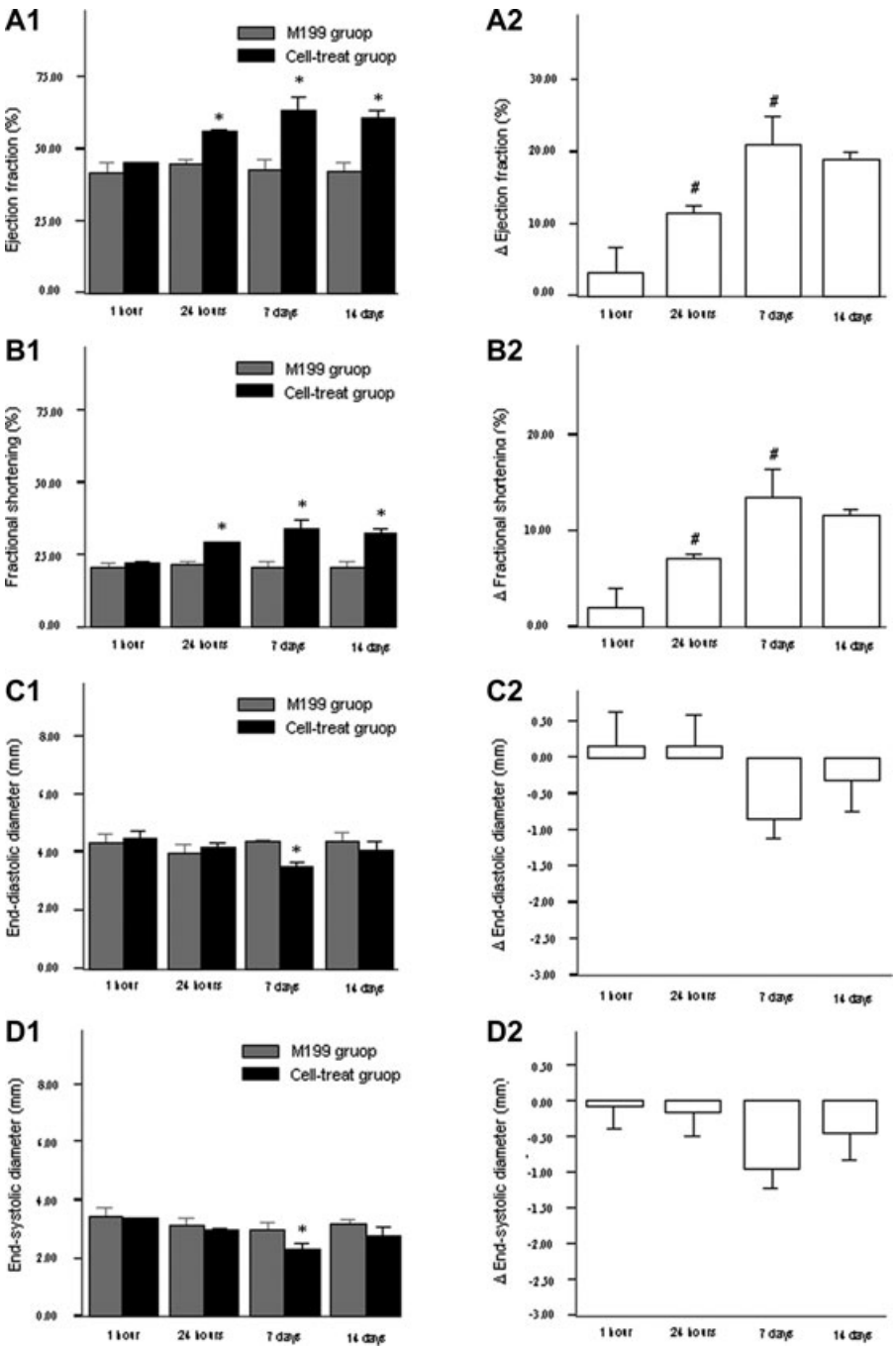

Fig. 3 The changes of cardiac function and left ventricular diameters after cell transplantation. (**A**1)–(**D**1) indicated the comparisons of cell transplantation (black column) and M199 transfer (grey column). (**A**2)–(**D**2) indicated the absolute changes of cardiac parameters from the control (M199 transfer). Bars mean standard errors. $*P < 0.05$ *versus* M199 injection group; $\#P < 0.05$ *versus* left neighbour.

that transplanted endothelium-committed or smooth muscle 22α-expressing cells, but not cardiac-committed cells induced a significant improvement of ejection fraction in mouse MI models. These finding indicated a functional contribution of the vascular cell fate decision of BMMNCs *in vivo*. Notably, mature endothelial cells possess limited regenerative capacity. There is therefore much interest in EPCs, an identified population of putative endothelial cell progenitors or angioblasts, especially into their purported role in postnatal neovascularization [21–22]. Previous experimental studies have demonstrated that EPCs administration partially rescued cardiovascular dysfunction following myocardial injury with some evidence for EPCs contribution to new vessel growth [23–24]. As a

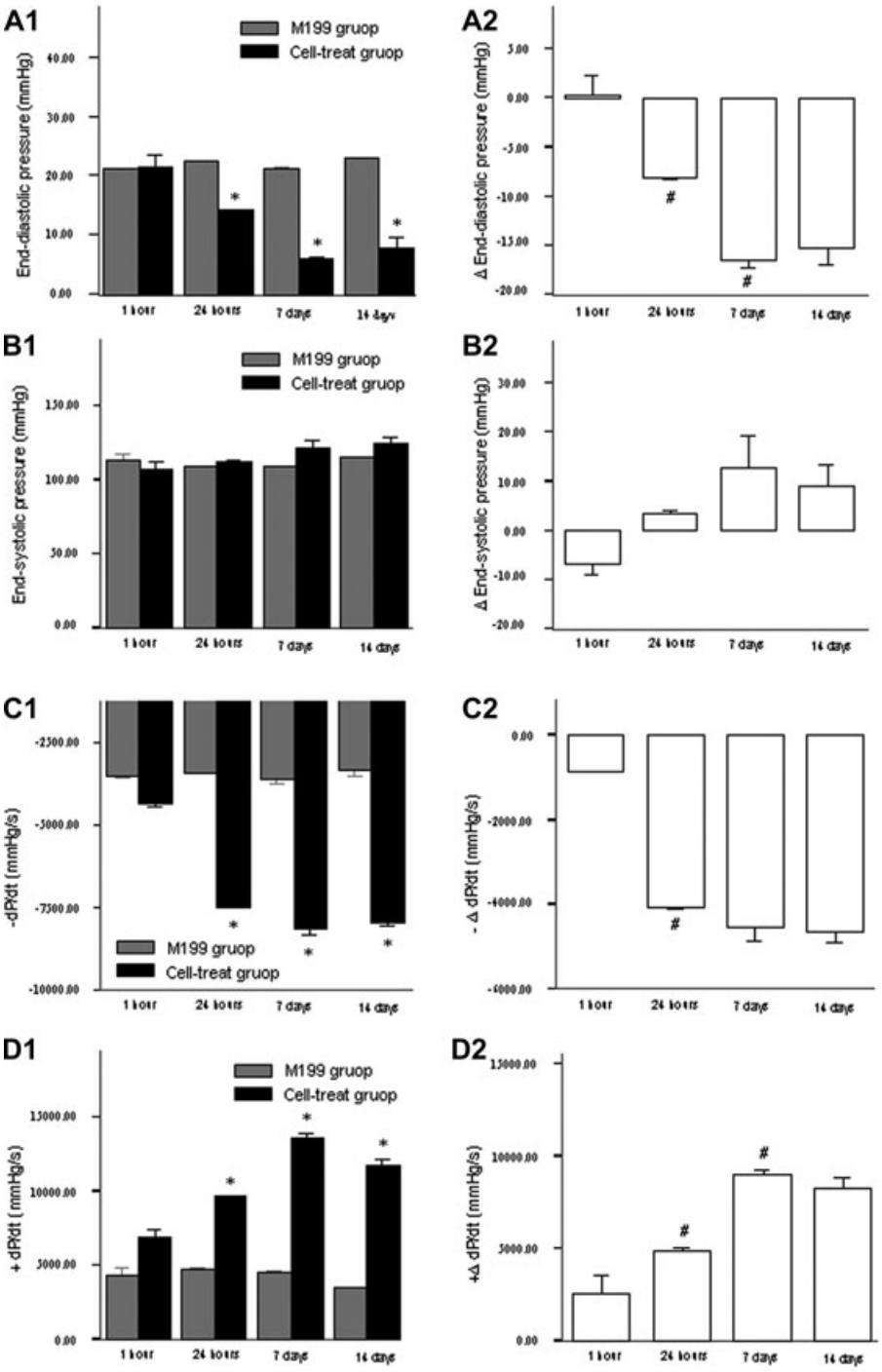

Fig. 4 The changes of left ventricular pressure after cell transplantation. (**A**1)–(**D**1) indicated the comparisons of cell transplantation (black column) and M199 transfer (grey column). (**A**2)–(**D**2) indicated the absolute changes of cardiac parameters from the control (M199 transfer). Bars mean standard errors. $*P < 0.05$ *versus* M199 injection group; $\#P < 0.05$ *versus* left neighbour.

result of these promising findings, this work focused on the commitments of BMMNCs to EPCs. On basis of these observations, we speculated that transplantation time-related angiogenesis in cell-inject zone might contribute to the transplantation time-related recovery of cardiac function after the infarction. Indeed, the present study indicated vessel density was in agreement with cardiac function associated with cell treatment at distinct time-points after MI. Unfortunately, fluorescence-labelled cells were not found in cell injection zone probably due to fluorescent quenching as a result of long period from cell injection to cell identification.

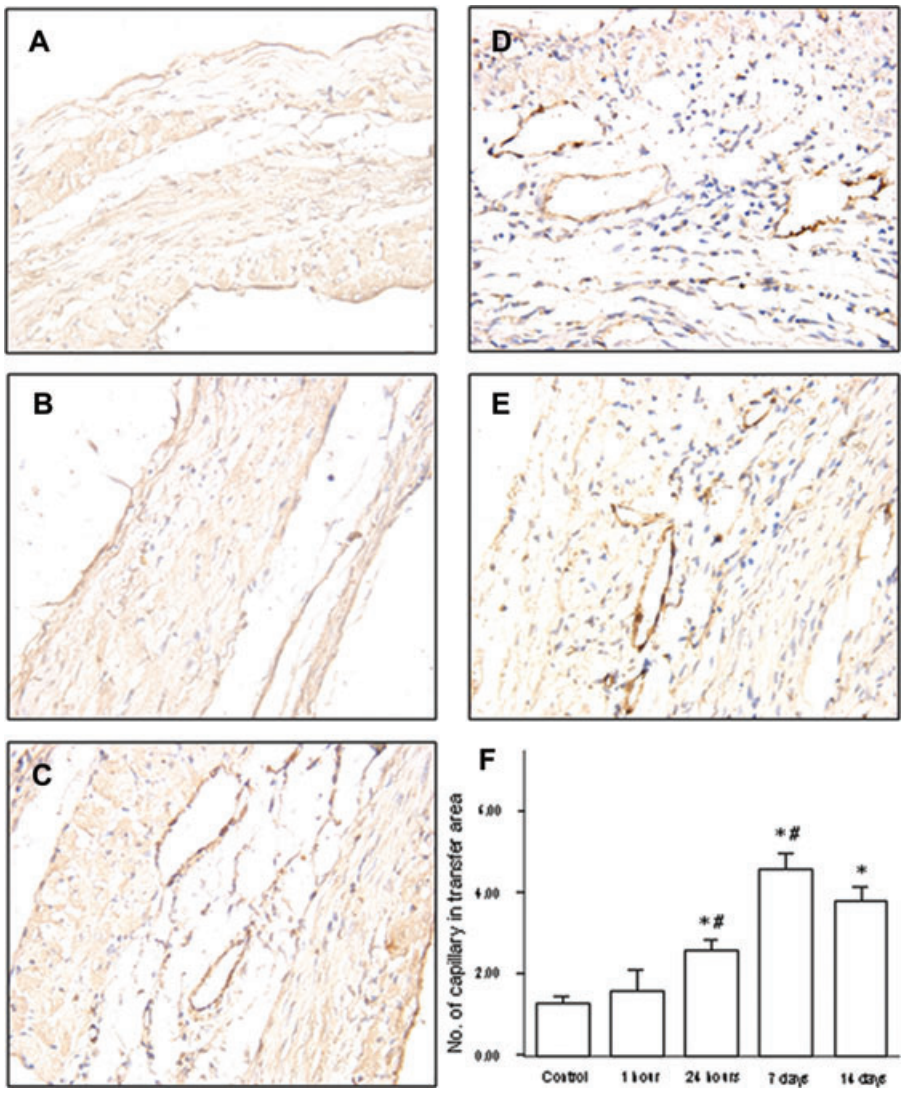

Fig. 5 Numeric density of vessels in myocardium from experimental groups at 8 weeks after MI. (**A**) M199 injection (the control); (**B**) cell therapy at hour 1 after the infarction; (**C**) cell therapy at hour 24 after the infarction; (**D**) cell therapy at day 7 after the infarction; (**E**) cell therapy at day 14 after the infarction. Bars mean S.D. $*P < 0.05$ *versus* the control group; $\#P < 0.05$ *versus* left neighbour.

Current researches trend to decipher the time-dependent therapeutic responses of cell treatment by time course of the production of cytokines or growth factors after MI, which were involved in survival and differentiation of the engrafted cells [1, 25–26]. However, the biochemical response within infarcted myocardium is an exceedingly complex network. The functional complexity of biological molecules greatly limited their use in elucidating the mechanism underlying the optimal timing of cell transfer for MI. Notably, our data fail to indicate the correlation between angiogenesis and serum VEGF level after MI, although it is well established that VEGF elicits a strong angiogenic response in a variety of *in vivo* models. That is to say, beneficial angiogenesis that promoted the improvement of cardiac function might be not attributable to VEGF-dependent angiogenic effects. It is natural to think of that there might exist other factors responsible for angiogenesis and subsequently impacting cell-based cardiac repair.

The effects of mechanical characteristics of the microenvironment around stem cells on their specifications have attracted a great attention. Matrix stiffness, corresponding to specific tissues, could promote tissue-mimetic differentiation of cells *in vitro* [27–28]. Notably, stiffness is also frequently altered in disease: sclerosis (as in atherosclerosis, osteosclerosis, etc.) literally means 'hardening'. Indeed, we here found the time-related changes in stiffness of infarcted myocardium from flexible to rigid, which were closely associated with the pathological tissue changes following MI. However, the knowledge for the effects of the mechanical changes was acquired scarcely. Recently, the stiffness-dependent effects of infarcted myocardium on directing cell development and biological function have been described. Isolated embryonic cardiomyocytes cultured on a series of flexible substrates showed that matrices that mimicked the stiffness (E ~ 11–17 kPa) of the developing myocardial microenvironment were

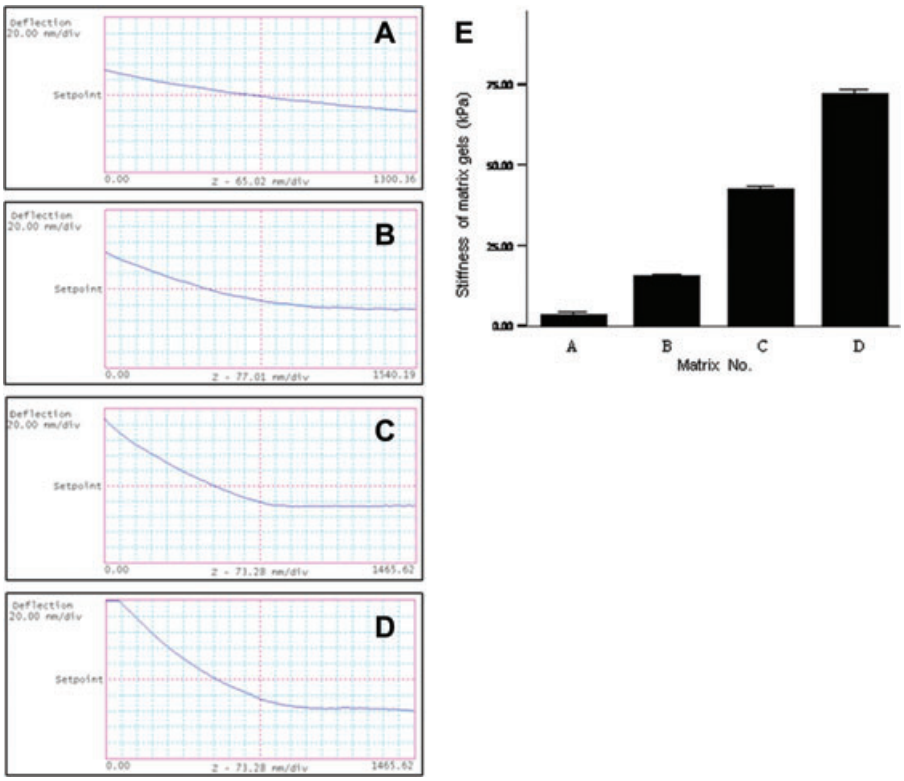

Fig. 6 *In vitro* mechanical mimicry of myocardium at different time-points after the infarction. (**A**) matrix gel with ~4 kPa stiffness, corresponding to infarcted myocardium at hour 24; (**B**) ~15 kPa, corresponding to that at hour 1; (**C**) ~42 kPa, corresponding to that at days 7 to 14; (**D**) ~72 kPa, corresponding to that at days 14 to 28. Bars mean S.D.

optimal for promoting actomyosin striation and cardiomyocytes beating. On hard matrices (E ~ 35–70 kPa) that mechanically mimicked a post-infarct fibrotic scar, cells overstrain themselves, lack striated myofibrils and stop beating [29]. Nevertheless, the functional details of mechanical microenvironment within infarcted myocardium have yet to be explored.

Specific to this work, the matrix substrate mechanically mimicking myocardium at 7 to 14 days after the infarction appeared to be optimal *in vitro* for inducing BMMNCs' specification to endothelial progenitor lineage. It implicated that there existed a time-related 'window' in myocardium stiffness suitable for engrafted cells' differentiation. And the time domains were basically consistent with the optimal timing of cell therapy for MI [1–2]. As described in the introduction and supported by the stiffness-directed lineage specification results above, the physical or mechanical conditions within infarcted myocardium might play an essential role in defining and deciphering the optimal time frame of cell treatment. However, the issue, how might cells 'feel' or sense tissue-like stiffness and transduce that information into lineage specification, remains unexplored. The available data suggest that integrin and non-muscle myosin II are likely to be involved in the matrix-elasticity sensing that drives lineage specification [5, 30]. Integrin, as the main receptors that connect the cytoskeleton to the extracellular matrix, mediates cell focal adhesion to sense the mechanical force [30] and regulates signalling pathways [31]. Subsequently, actin cytoskeletons were assembled or disassembled under regulations of altering non-muscle myosin II expression [5]. The process is necessary to cell specification. The potential effects of integrin and non-muscle myosin II on mediating stiffness-dependent commitment to endothelial progenitor lineages should be further investigated in future work, and understanding their influence probably provides new insight into the rationale and mechanism of cell-based regeneration.

Traditional views trend to use the time-related changes in cytokines or growth factors possibly impacting engrafted cells' differentiation to explain the potential mechanism underlying the optimal time domains. However, the biochemical response within infarcted myocardium is an exceedingly complex network. Although some chemokines may certainly benefit the engrafted cells, the majority of them might be deleterious for survival and differentiation of cells [32]. Even the same cytokines often have paradoxical effects or counteract each other [33–34]. The functional complexity of these cytokines greatly limited their use in elucidating the mechanism underlying the optimal timing of cell transfer for MI. Unexpectedly, in this work neither higher concentration (10–20 ng/ml) of VEGF nor free VEGF, but lower concentrations (2.5 ng/ml) of VEGF, exerted at utmost the functions of promoting specification of BMMNCs along EPCs. Mechanically, under conditions of flexible culture substrates, higher concentration (20 ng/ml) of VEGF might inhibit biological behaviours and veil functional differences of BMMNCs among varied stiffness. And lower concentration of environmental VEGF might not inhibit VEGF or other cytokines secretion

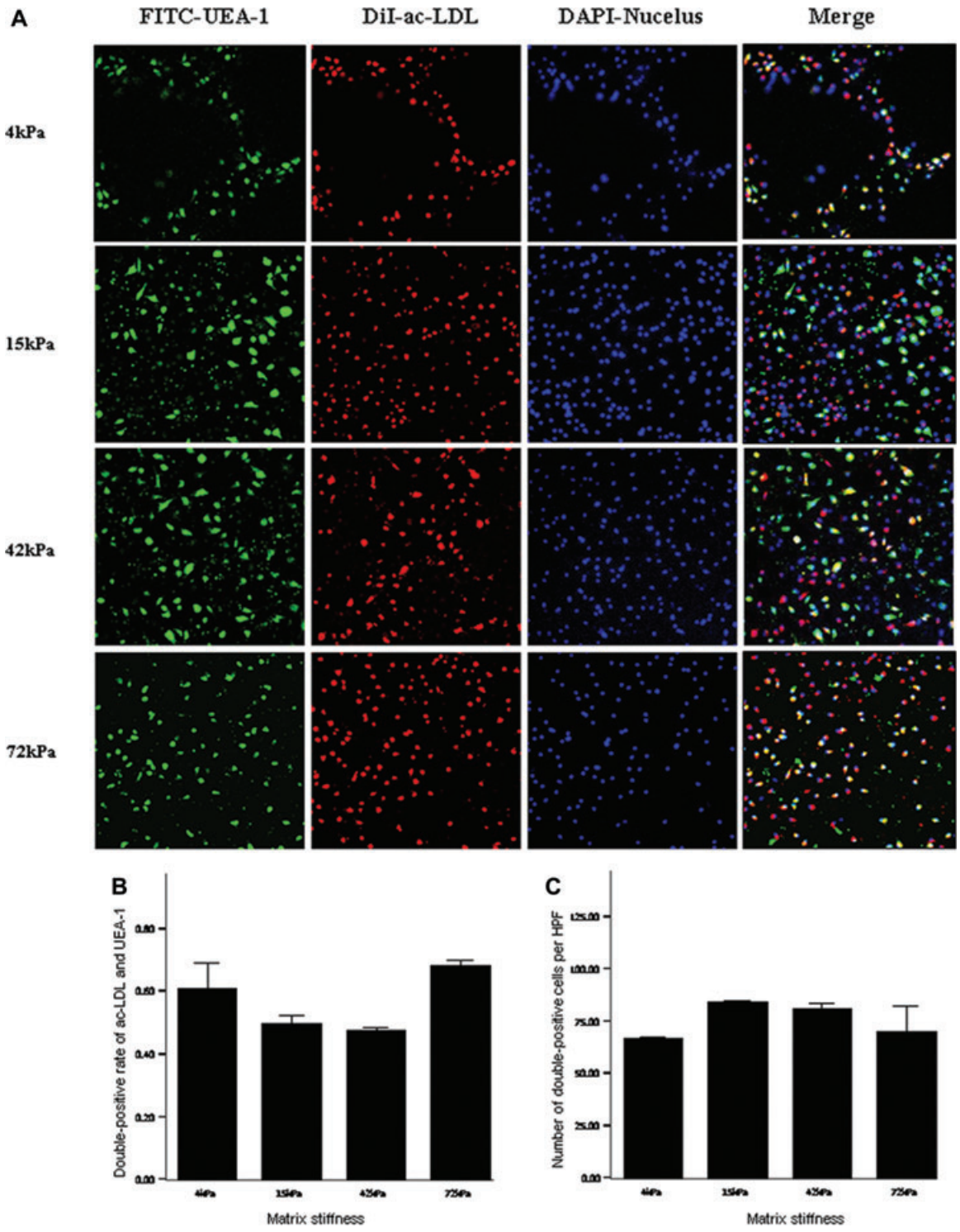

Fig. 7 Double-positive cells for DiI-acLDL uptake and FITC-UEA-1 binding on the substrates with varied stiffness under culture conditions of 20 ng/ml VEGF. (**A**) direct fluorescent staining; (**B**) comparisons of rates of double-positive cells; (**C**) comparisons of numbers of double-positive cells per HPF. Bars mean S.D. FITC-UEA-1: FITC-labelled ulex europaeus agglutinin I lectin; DiI-acLDL: DiI-labelled acetylated low-density lipoprotein. HPF: high power field. All *P*-values >0.05.

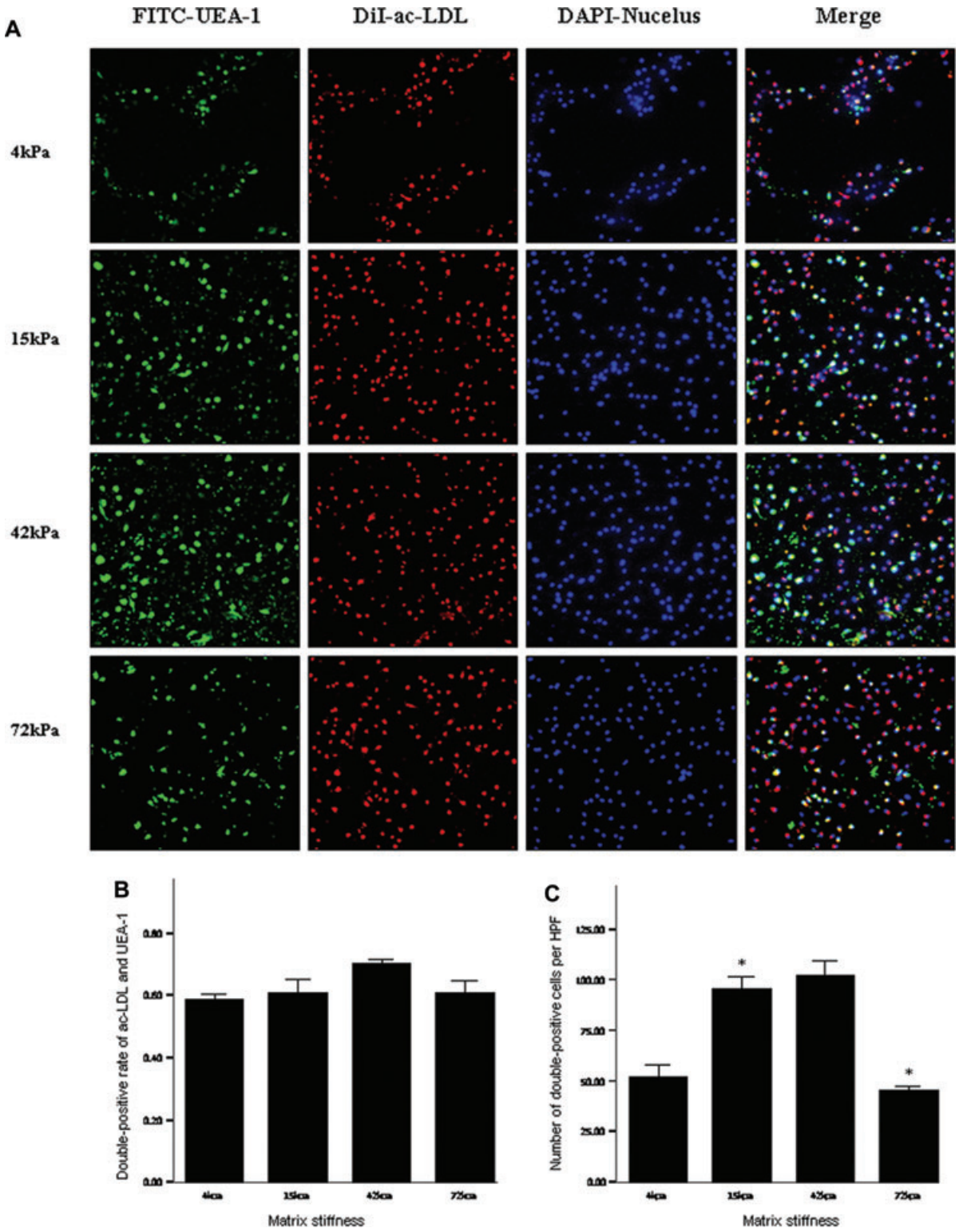

Fig. 8 Double-positive cells for DiI-acLDL uptake and FITC-UEA-1 binding on the substrates with varied stiffness under culture conditions of 10 ng/ml VEGF. $^{*}P < 0.05$ *versus* left neighbour. Footnotes as Figure 7.

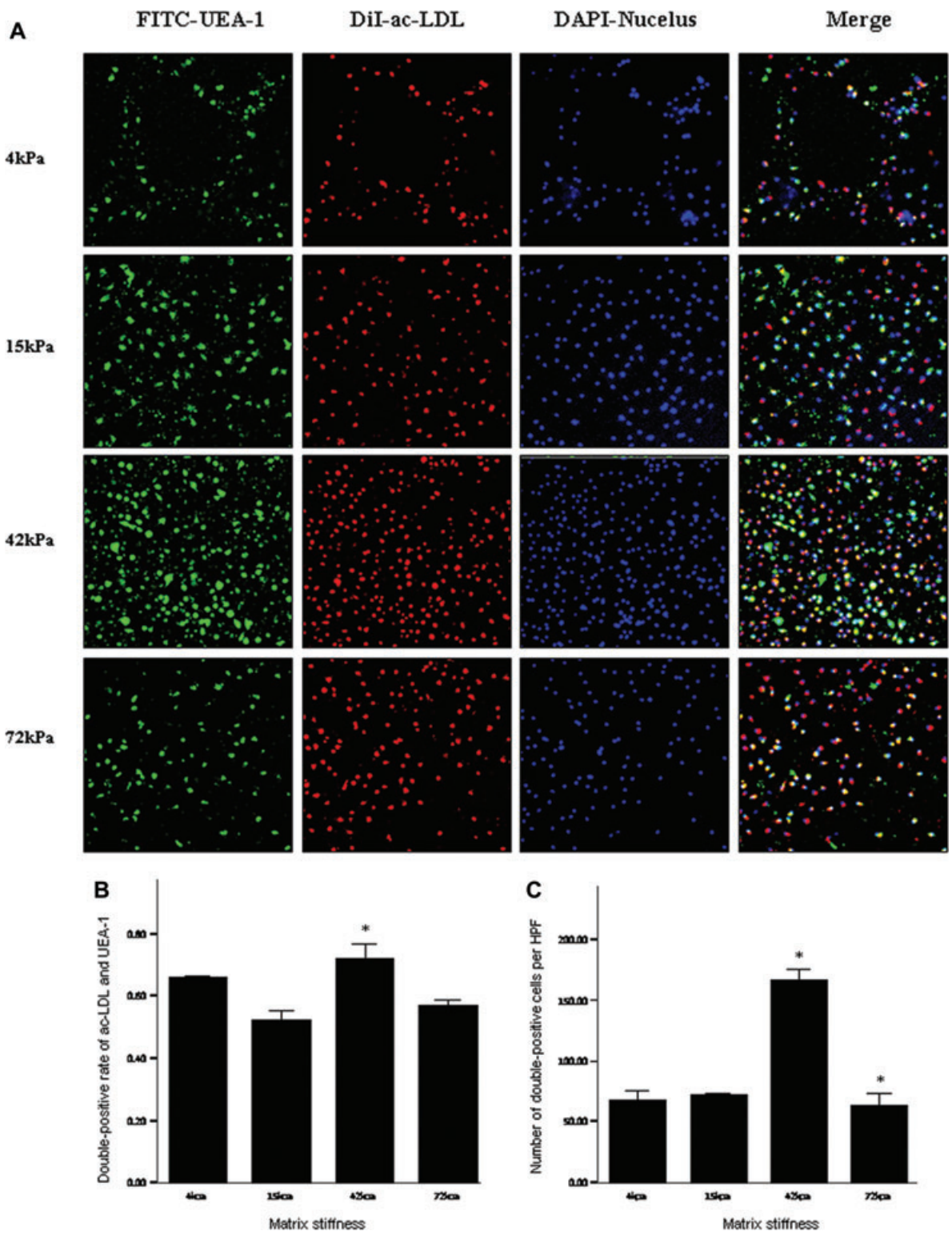

Fig. 9 Double-positive cells for DiI-acLDL uptake and FITC-UEA-1 binding on the substrates with varied stiffness under culture conditions of 2.5 ng/ml VEGF. $^{*}P < 0.05$ *versus* left neighbour. Footnotes as Figure 7.

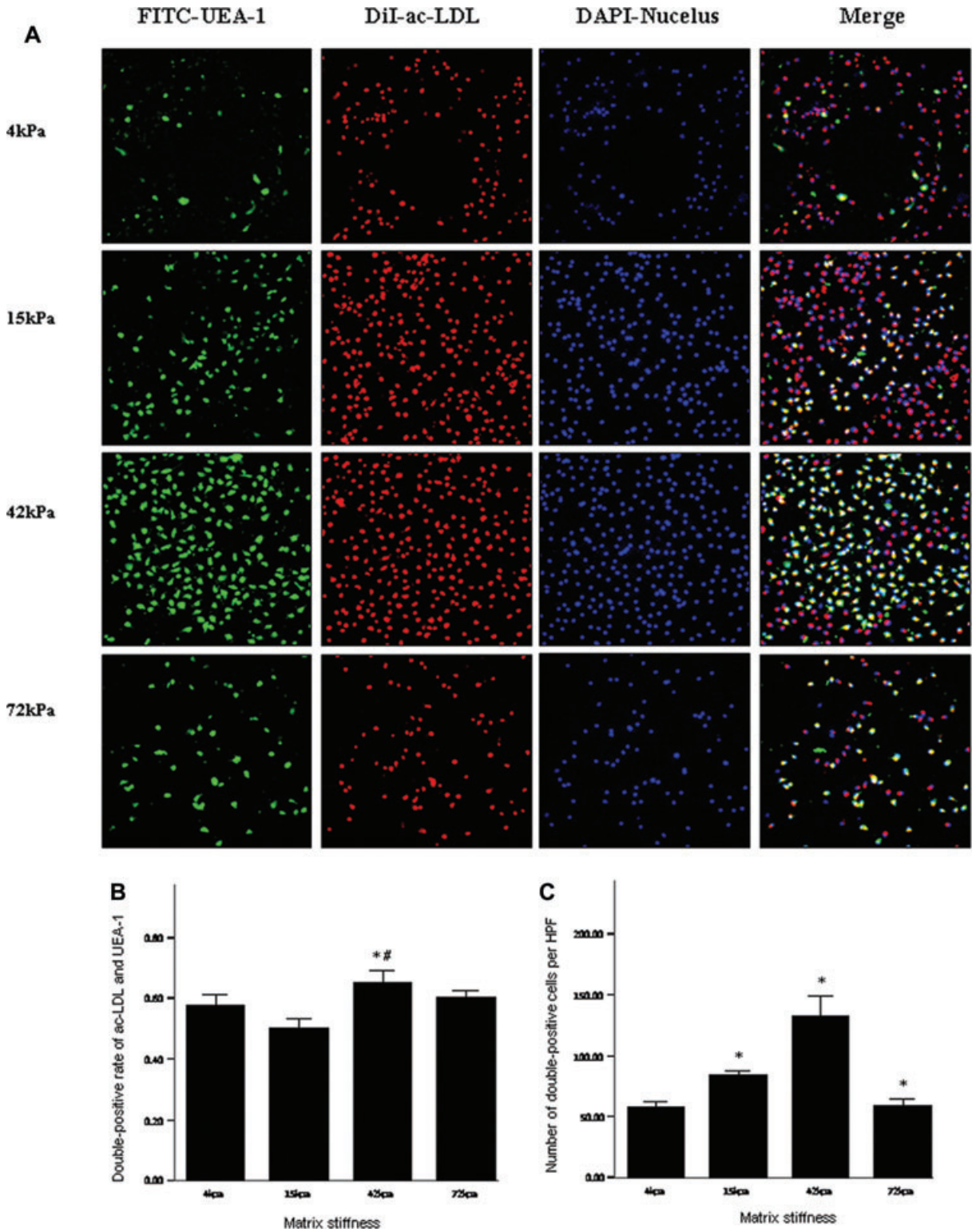

Fig. 10 Double-positive cells for DiI-acLDL uptake and FITC-UEA-1 binding on the substrates with varied stiffness under culture conditions of 10 ng/ml VEGF. $*P < 0.01$ *versus* left neighbour. $\#P = 0.01$ *versus* 4 kPa group. Footnotes as Figure 7.

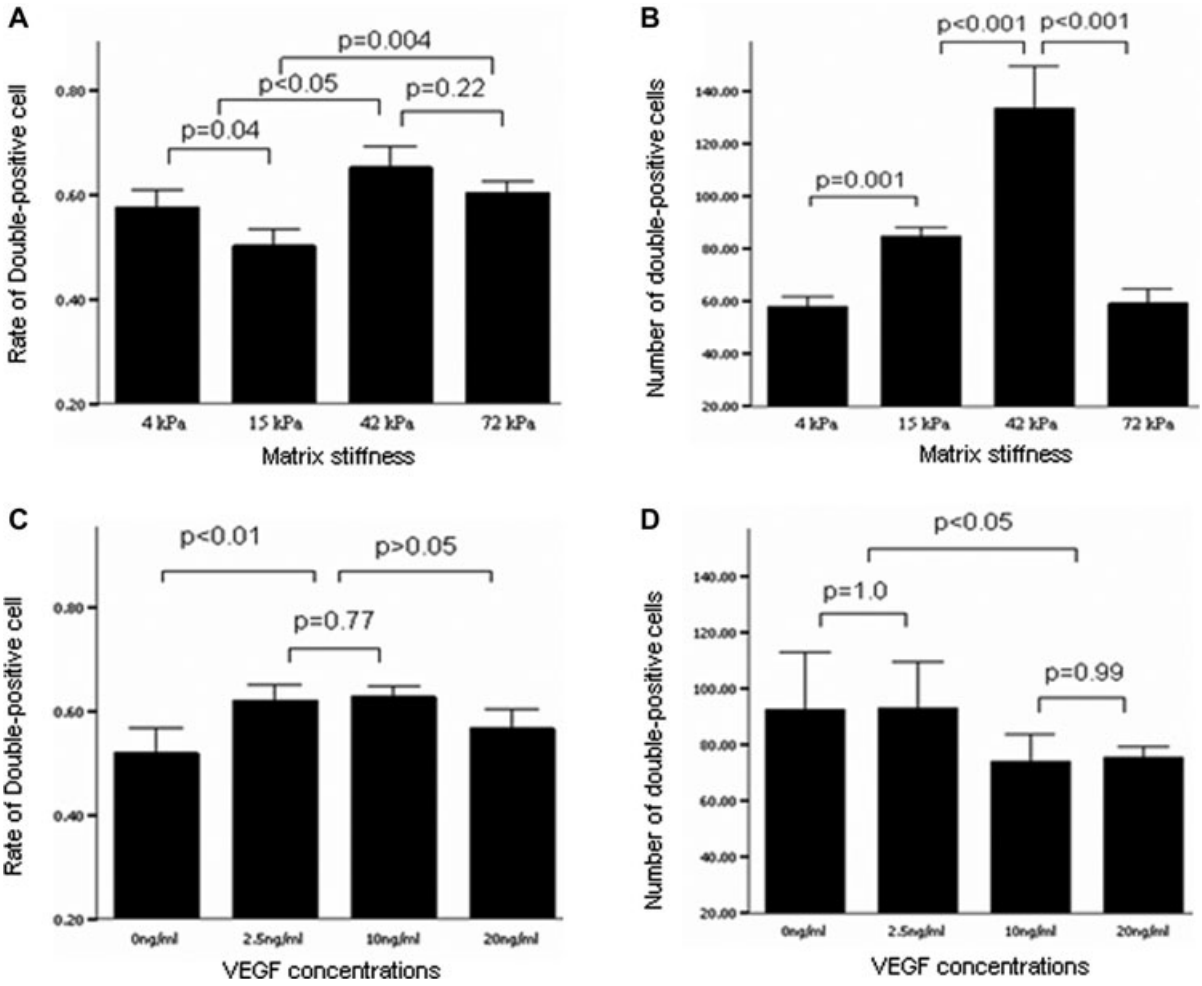

Fig. 11 Two-way analysis of variance for effect of matrix elasticity (**A**, **B**) and VEGF concentration (**C**, **D**) on the percentages (**A**, **C**) and numbers (**B**, **D**) of double-positive cells for DiI-acLDL uptake and FITC-UEA-1 binding. Bars mean S.D. VEGF: vascular endothelial growth factor.

of committed EPCs and this in turn promoted BMMNCs' differentiation to EPCs. Indeed, inter-stiffness effect differences reached maximum size when VEGF was removed from cell culture medium. The interesting result suggested VEGF concentration greatly affected functional exertion of tissue-like stiffness. There might exist a co-effect of matrix stiffness and VEGF concentration on cell lineage specification. Extremely limited information on the interaction between mechanical factors and biological factors with potential functions of inducing cells' differentiation could be available. Hinz and co-workers found *in vitro* that cell-generated mechanical tension results in release of active transforming growth factor-β from stiff extracellular matrix, providing a mechanism for differentiation and maintenance of myofibroblasts [35]. Nevertheless, the potential mechanism underlying BMMNCs specification co-induced by physical and biological factors deserves further detailed investigation.

It is noteworthy that these results here were obtained on flexible cell culture substrates and could not be extrapolated to those on regular culture dishes. Regular culture system with rigid substrate could not mimic the physical or mechanical microenvironment around cultured cells, which limited the displays of real biological functions of them. Thus, physical characteristics of culture substrates should be fully considered in the culture and assessment of biological behaviours of stem or progenitor cells. The results here have significant implications for understanding physical effects of the *in vivo* microenvironment and also for therapeutic uses of stem cells. Based on the current observations that excessive rigidification seems likely to limit cell-based cardiac repair by limiting favourable phenotype specification, our work also highlights the need for optimizing matrix elasticity to foster regeneration, which seems applicable to a number of regenerative applications of stem cells.

Current observations contribute to understand the mechanism underlying the optimal timing of BMMNCs transplantation after MI. More importantly, these patients with missed opportunity for cell transplantation will still be able to achieve benefits from cell

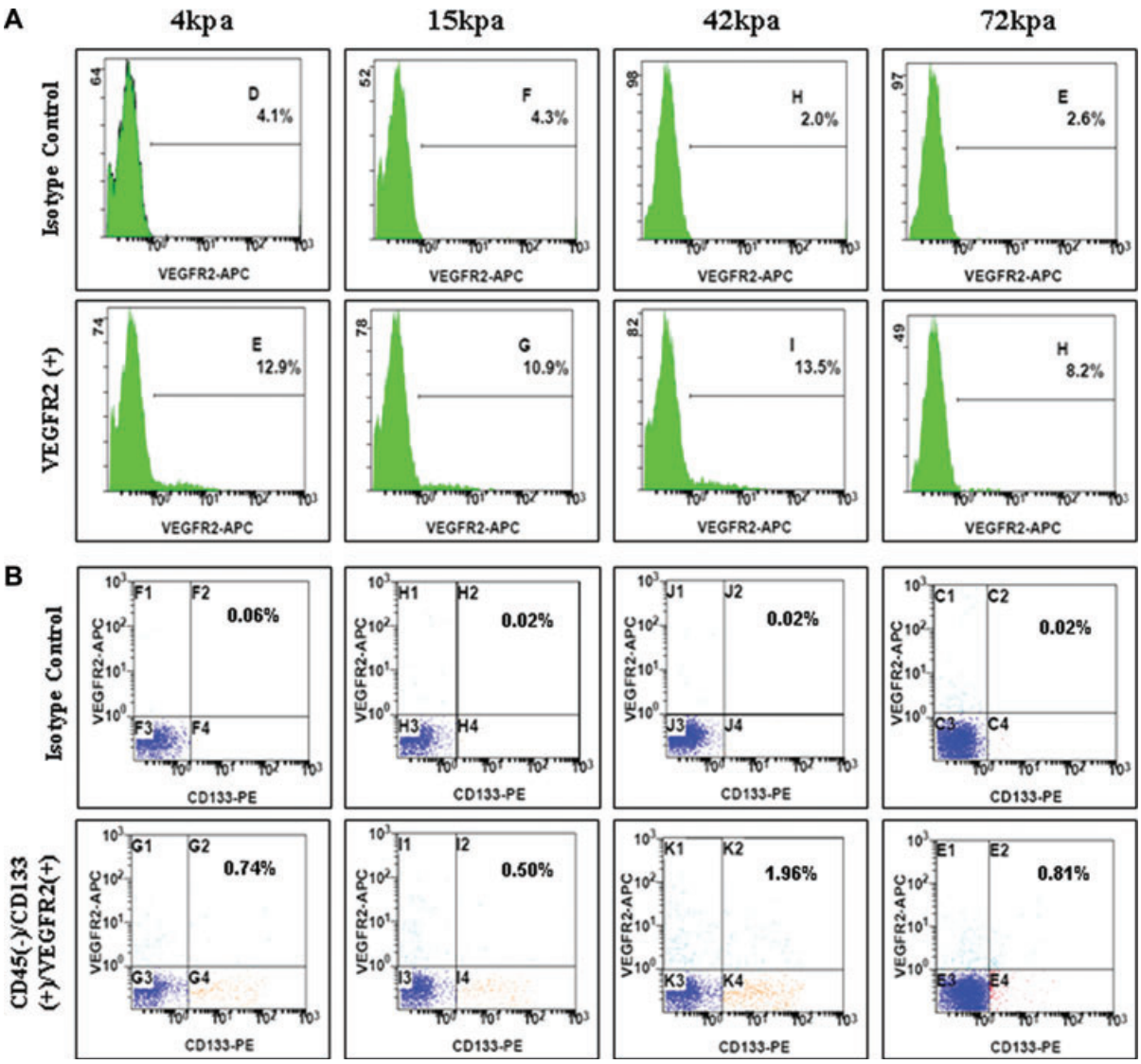

Fig. 12 Flow cytometry for expressions of EPC-specific antigens in lower concentration VEGF. (**A**) Expression of VEGFR2$^+$; (**B**) combined expression of VEGFR2$^+$, CD133$^+$ and CD45$^-$.

therapy by attenuating cardiac remodelling and consequently changing myocardial stiffness after the infarction. Cell transplantation in combination with anti-remodelling treatment might bring a more beneficial effect to these patients than the procedure alone.

Acknowledgements

The study was supported by Youth Science Funds of Zhongshan hospital (KB363), Research Fund for the Doctoral Program of Higher Education (20100071120074), Youth Science Funds of National Natural Science Foundation (30900600 and 30700318), Shanghai Scientific Research Fund (06DJ14001), Program for Shanghai Outstanding Medical Academic Leader (LJ06008) and National Basic Research Program of China (2006CB943704). The authors thank Dr. Kai Hu from W¸rzburg University, Germany, for his help in proofreading and editing this manuscript and Dr. Huiqin Li from Instrumental Analysis Center, Shanghai Jiaotong University, China, for the help of atomic force microscopy-based force measurements of polyacrylamide gels and myocardial tissue.

Conflict of interest

The authors confirm that there are no conflicts of interest.

References

1. **Bartunek J, Wijns W, Heyndrickx GR, *et al.*** Timing of intracoronary bone-marrow-derived stem cell transplantation after ST-elevation myocardial infarction. *Nat Clin Pract Cardiovasc Med.* 2006; 3: S52–6.
2. **Hu XY, Wang JN, Chen J, *et al.*** Optimal temporal delivery of bone marrow mesenchymal stem cells in rats with myocardial infarction. *Eur J Cardiothorac Surg.* 2007; 31: 438–43.
3. **Schachinger V, Erbs S, Elsasser A, *et al.*** Intracoronary bone marrow-derived progenitor cells in acute myocardial infarction. *N Engl J Med.* 2006; 355: 1210–21.
4. **Zhang S, Sun A, Xu D, *et al.*** Impact of timing on efficacy and safetyof intracoronary autologous bone marrow stem cells transplantation in acute myocardial infarction: a pooled subgroup analysis of randomized controlled trials. *Clin Cardiol.* 2009; 32: 458–66.
5. **Engler AJ, Sen S, Sweeney HL, *et al.*** Matrix elasticity directs stem cell lineage specification. *Cell.* 2006; 126: 677–89.
6. **Gao XM, Xu Q, Kiriazis H, *et al.*** Mouse model of post-infarct ventricular rupture: time course, strain- and gender-dependency, tensile strength, and histopathology. *Cardiovasc Res.* 2005; 65: 469–77.
7. **Berry MF, Engler AJ, Woo YJ, *et al.*** Mesenchymal stem cell injection after myocardial infarction improves myocardial compliance. *Am J Physiol Heart Circ Physiol.* 2006; 290: H2196–203.
8. **Zhang S, Sun A, Liang Y, *et al.*** A role of myocardial stiffness in cell-based cardiac repair: a hypothesis. *J Cell Mol Med.* 2009; 13: 660–3.
9. **Patten RD, Aronovitz MJ, Deras-Mejia L, *et al.*** Ventricular remodeling in a mouse model of myocardial infarction. *Am J Physiol.* 1998; 274: H1812–20.
10. **Boyum A, Lovhaug D, Tresland L, *et al.*** Separation of leucocytes: improved cell purity by fine adjustments of gradient medium density and osmolality. *Scand J Immunol.* 1991; 34: 697–712.
11. **Nishio R, Sasayama S,Matsumori A.** Left ventricular pressure-volume relationship in a murine model of congestive heart failure due to acute viral myocarditis. *J Am Coll Cardiol.* 2002; 40: 1506–14.
12. **Domke J, Radmacher M.** Measuring the elastic properties of thin polymer films with the atomic force microscope. *Langmuir.* 1998; 14: 3320–5.
13. **Pelham RJ, Wang YL.** Cell locomotion and focal adhesions are regulated by substrate flexibility. *Proc Natl Acad Sci USA.* 1997; 94: 13661–5.
14. **Wang YL, Pelham RJ Jr.** Preparation of a flexible, porous polyacrylamide substrate for mechanical studies of cultured cells. *Methods Enzymol.* 1998; 298: 489–96.
15. **Kalka C, Masuda H, Takahashi T, *et al.*** Transplantation of *ex vivo* expanded endothelial progenitor cells for therapeutic neovascularization. *Proc Natl Acad Sci USA.* 2000; 97: 3422–7.
16. **Korbling M, Estrov Z.** Adult stem cells for tissue repair – A new therapeutic concept? *N Engl J Med.* 2003; 349: 570–82.
17. **van der Bogt KE, Sheikh AY, Schrepfer S, *et al.*** Comparison of different adult stem cell types for treatment of myocardial ischemia. *Circulation.* 2008; 118: S121–9.
18. **Janssens S, Dubois C, Boyaert J, *et al.*** Autologous bone marrow-derived stem-cell transfer in patients with ST-segment elevation myocardial infarction: double-blind, randomised controlled trial. *Lancet.* 2006; 367: 113–21.
19. **Silvestre JS, Tamarat R, Ebrahimian TG, *et al.*** Vascular endothelial growth factor-B promotes *in vivo* angiogenesis. *Circ Res.* 2003; 93: 114–23.
20. **Yoon CH, Koyanagi M, Iekushi K, *et al.*** Mechanism of improved cardiac function after bone marrow mononuclear cell therapy: role of cardiovascular lineage commitment. *Circulation.* 2010; 121: 2001–11.
21. **Asahara T, Murohara T, Sullivan A, *et al.*** Isolation of putative progenitor endothelial cells for angiogenesis. *Science.* 1997; 275: 964–7.
22. **Shantsila E, Watson T, Lip GYH.** Endothelial progenitor cells in cardiovascular disorders. *J Am Coll Cardiol.* 2007; 49: 741–52.
23. **Rafii S, Lyden D.** Therapeutic stem and progenitor cell transplantation for organ vascularization and regeneration. *Nat Med.* 2003; 9: 702–12.
24. **Kocher AA, Schuster MD, Szabolcs MJ, *et al.*** Neovascularization of ischemic myocardium by human bone-marrow-derived angioblasts prevents cardiomyocyte apoptosis, reduces remodeling and improves cardiac function. *Nat Med.* 2001; 7: 430–6.
25. **Kamihata H, Matsubara H, Nishiue T, *et al.*** Implantation of bone marrow mononuclear cells into ischemic myocardium enhances collateral perfusion and regional function *via* side supply of angioblasts, angiogenic ligands, and cytokines. *Circulation.* 2001; 104: 1046–2.
26. **Bartunek J, Vanderheyden M, Vandekerckhove B, *et al.*** Intracoronary injection of CD133-positive enriched bone marrow progenitor cells promotes cardiac recovery after recent myocardial infarction – feasibility and safety. *Circulation.* 2005; 112: I178–83.
27. **Engler AJ, Griffin MA, Sen S, *et al.*** Myotubes differentiate optimally on substrates with tissue-like stiffness: pathological implications for soft or stiff microenvironments. *J Cell Biol.* 2004; 166: 877–87.
28. **Discher DE, Janmey P, Wang YL.** Tissue cells feel and respond to the stiffness of their substrate. *Science.* 2005; 310: 1139–43.
29. **Engler AJ, Carag-Krieger C, Johnson CP, *et al.*** Embryonic cardiomyocytes beat best on a matrix with heart-like elasticity: scar-like rigidity inhibits beating. *J Cell Sci.* 2008; 121: 3794–802.
30. **Katsumi A, Orr AW, Tzima E, Schwartz MA.** Integrins in mechanotransduction. *J Biol Chem.* 2004; 279: 12001–4.
31. **Schwartz MA, Assoian RK.** Integrins and cell proliferation: regulation of cyclin-dependent kinases *via* cytoplasmic signaling pathways. *J Cell Sci.* 2001; 114: 2553–60.
32. **Fibbe WE, Pruijt JFM, van Kooyk Y, *et al.*** The role of metalloproteinases and adhesion molecules in interleukin-8-induced stem-cell mobilization. *Semin Hematol.* 2000; 37: 19–24.
33. **Nian M, Lee P, Khaper N, *et al.*** Inflammatory cytokines and postmyocardial infarction remodeling. *Circ Res.* 2004; 94: 1543–53.
34. **Vandervelde S, van Luyn MJA, Tio RA, *et al.*** Signaling factors in stem cell-mediated repair of infarcted myocardium. *J Mol Cell Cardiol.* 2005; 39: 363–76.
35. **Wipff PJ, Rifkin DB, Meister JJ, *et al.*** Myofibroblast contraction activates latent TGF-beta1 from the extracellular matrix. *J Cell Biol.* 2007; 179: 1311–23.